

# Effect of High Aircraft Tire Pressure on Flexible Pavements: Near- Surface Damage

---

Hao Wang

Imad L. Al-Qadi

*University of Illinois at Urbana-Champaign*



# Outline

---

- **Introduction**
- **Objective and Scope**
- **Development of 3-D FE Model**
  - Simulation of tire loading
  - Material characterization
- **Analysis and Results**
  - Effect of contact pressure on pavement responses
  - Effect of high tire pressure on pavement responses
- **Summary**

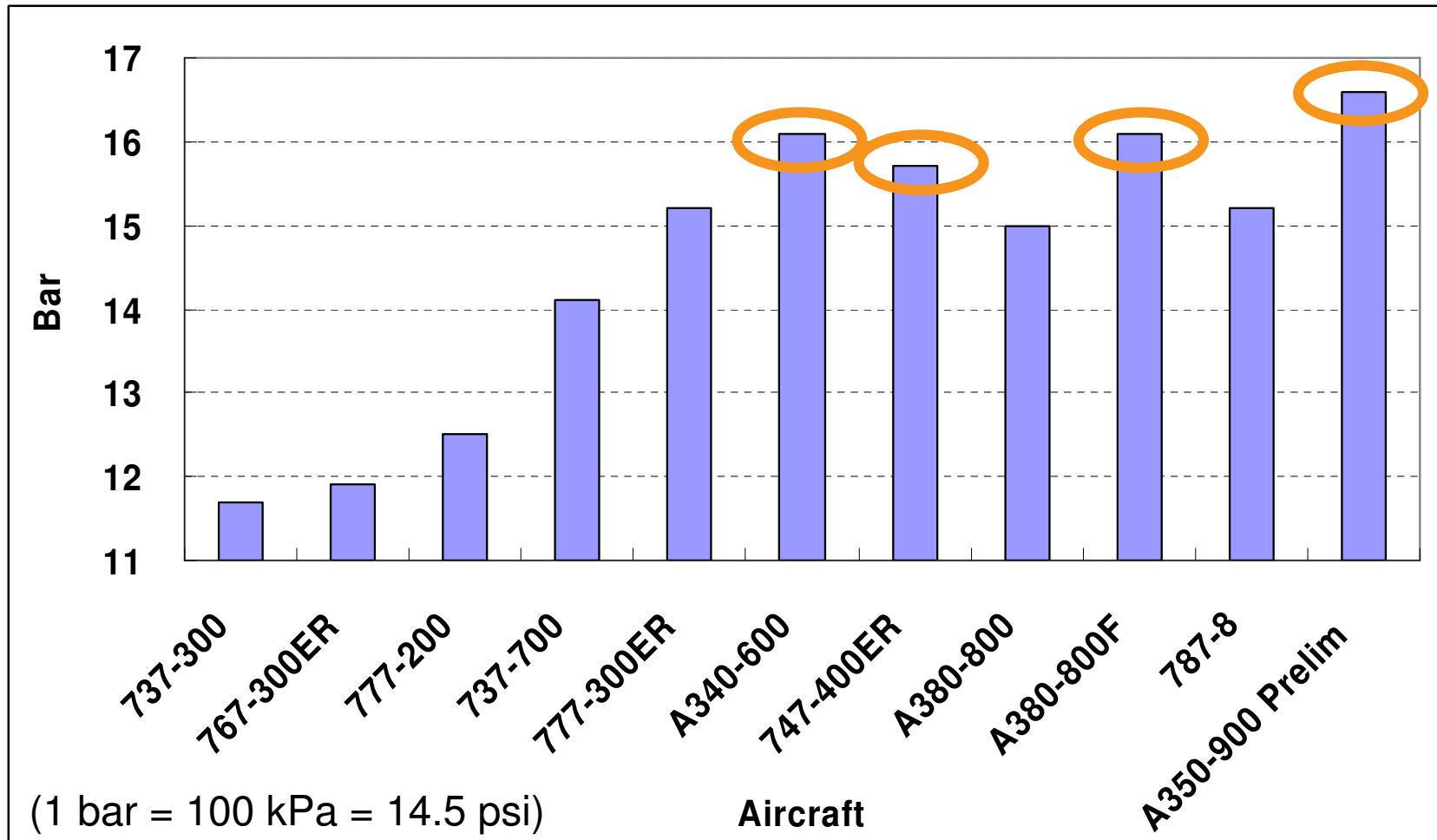


# Introduction

---

- **Four tire pressure categories (W / X / Y / Z) in ACN/PCN system (ICAO, 1981)**
  - W – no pressure limitation – high
  - X – 15 bars limitation – medium
  - Y – 10 bars limitation – low
  - Z – 5 bars limitation – very low
- **Current pavement capacity and new aircraft generation are not considered**
- **The use of W and X categories is not clearly defined**

# Aircraft Tire Pressure Trend



(After C. Fabre, 2009)



# Effect of High Tire Pressure

---

- **High truck-tire pressure increases flexible pavement damage. It is affected by**
  - Load and tire-pressure levels
  - Pavement structure
  - Response type
  - Response location
- **Boeing high tire pressure test at FAA NAPTF**
  - High tire pressure @ 16.5 bars and 50-kip loading
  - Rutting is found as the main failure mode
- **Airbus HTPT program**

# Mechanistic Analysis of Pavement Responses

---

- ❑ **Elastic layer theory is used in conventional pavement design**
- ❑ **Limitations of elastic layer theory**
  - ❑ Static circular uniform pressure distribution is inconsistent with real tire loading
  - ❑ Effects of tire speed and loading frequency are not considered
  - ❑ HMA viscoelasticity may not be fully considered



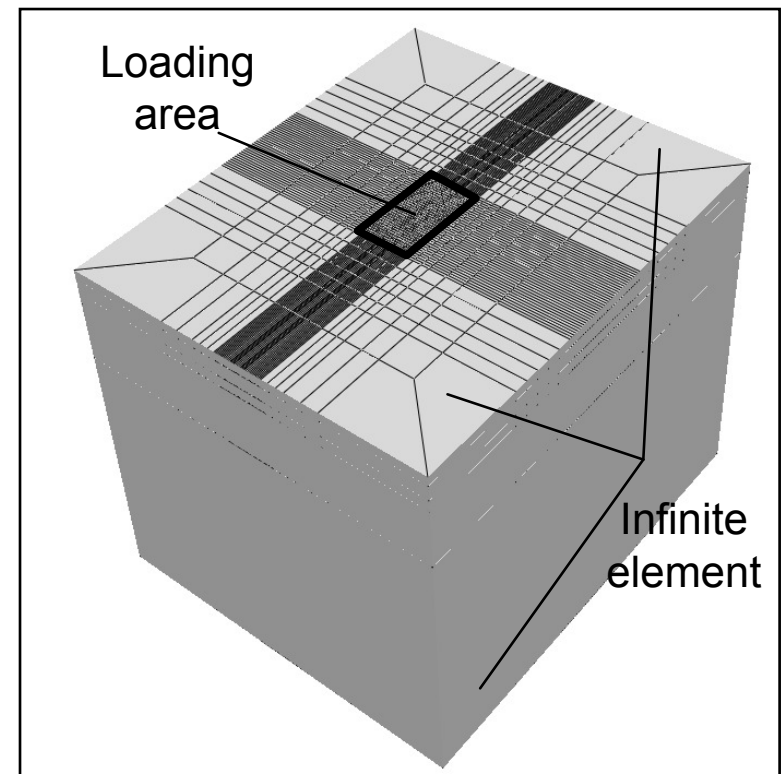
# Objective and Scope

---

- ❑ **Develop a 3-D FE pavement model under aircraft tire loading**
  - ❑ Simulation of tire loading
  - ❑ Material characterization
- ❑ **Analyze effects of contact stress and high tire pressure on pavement responses**
  - ❑ Two tire pressure levels (also assuming different contact stress distributions)
  - ❑ Two different base supports

# 3-D Finite Element Modeling

- **3-D FE model is used to capture**
- Non-uniform contact pressure
- Moving tire load
- Implicit dynamic analysis
- Viscoelastic HMA layer
- Infinite boundaries

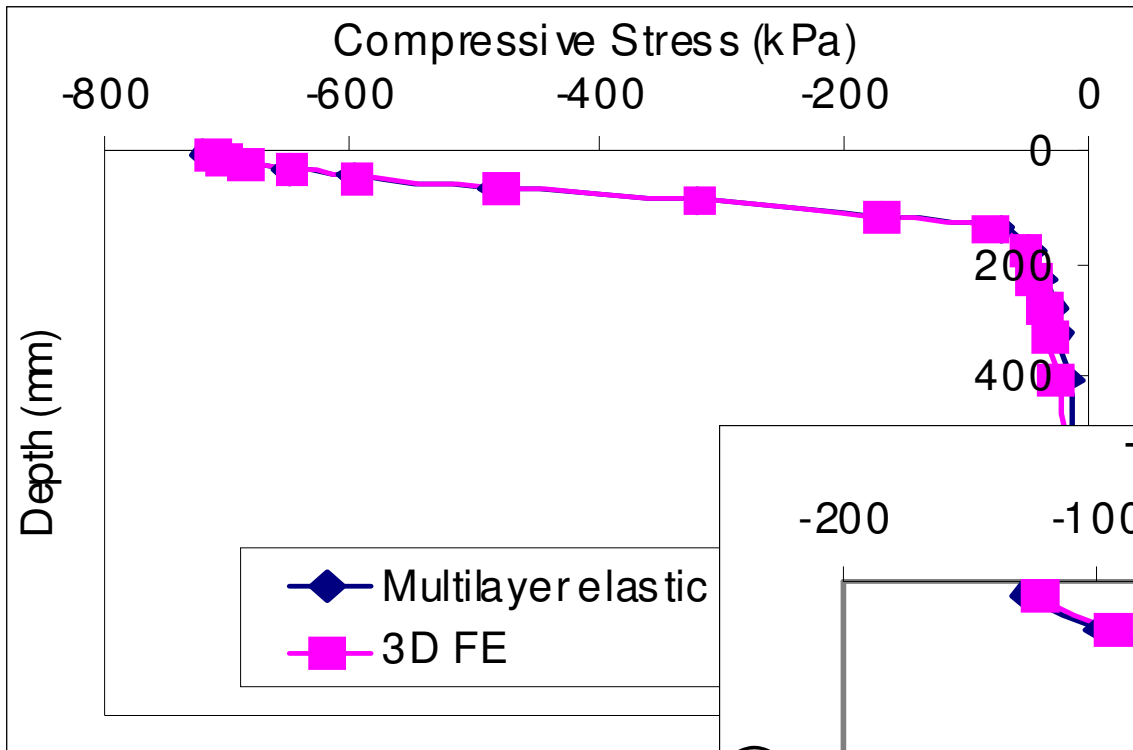


# Element Size and Boundary Conditions

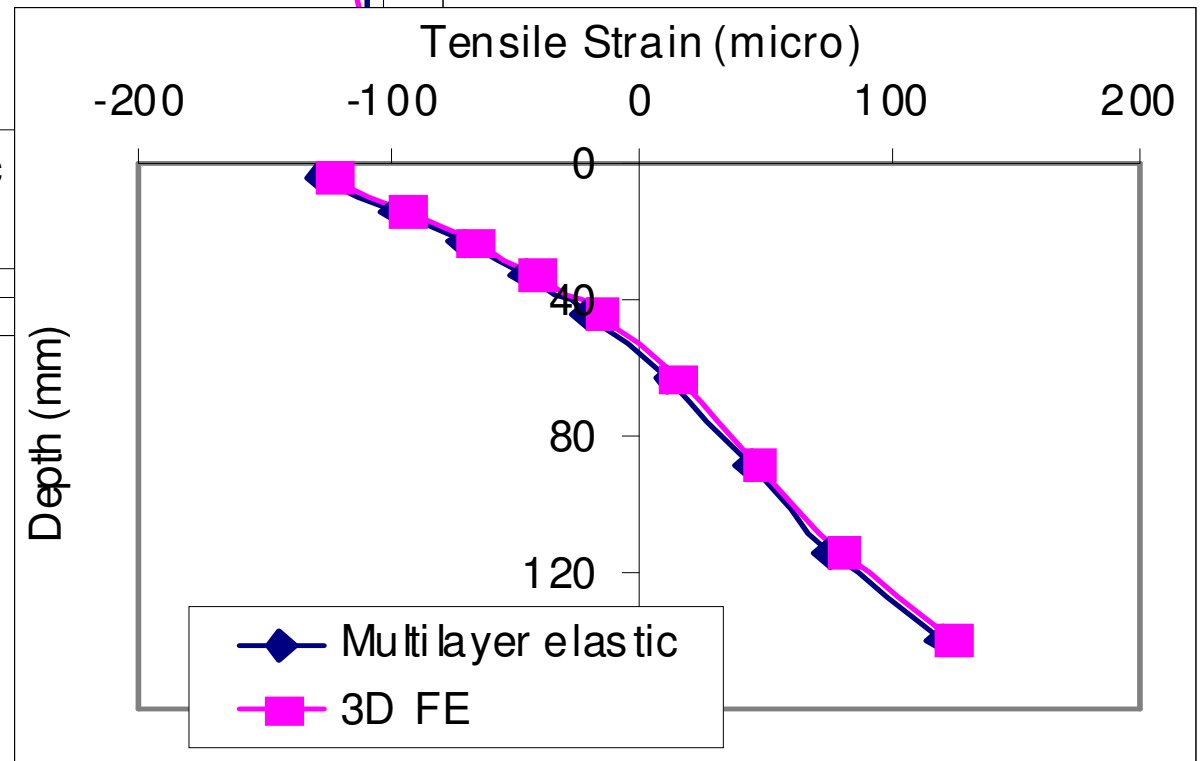
---

- ❑ **Element vertical size:**
  - ❑ 9.5 mm for HMA layer
  - ❑ 30-50 mm for base layer
  
- ❑ **Element horizontal dimension:**
  - ❑ 10-20 mm in the transverse direction
  - ❑ 40 mm in the longitudinal (moving) direction
  
- ❑ **Infinite elements used to reduce degrees of freedom and create “silent” boundaries**
  
- ❑ **Coulomb frictional interfaces are used**

# Model Verification

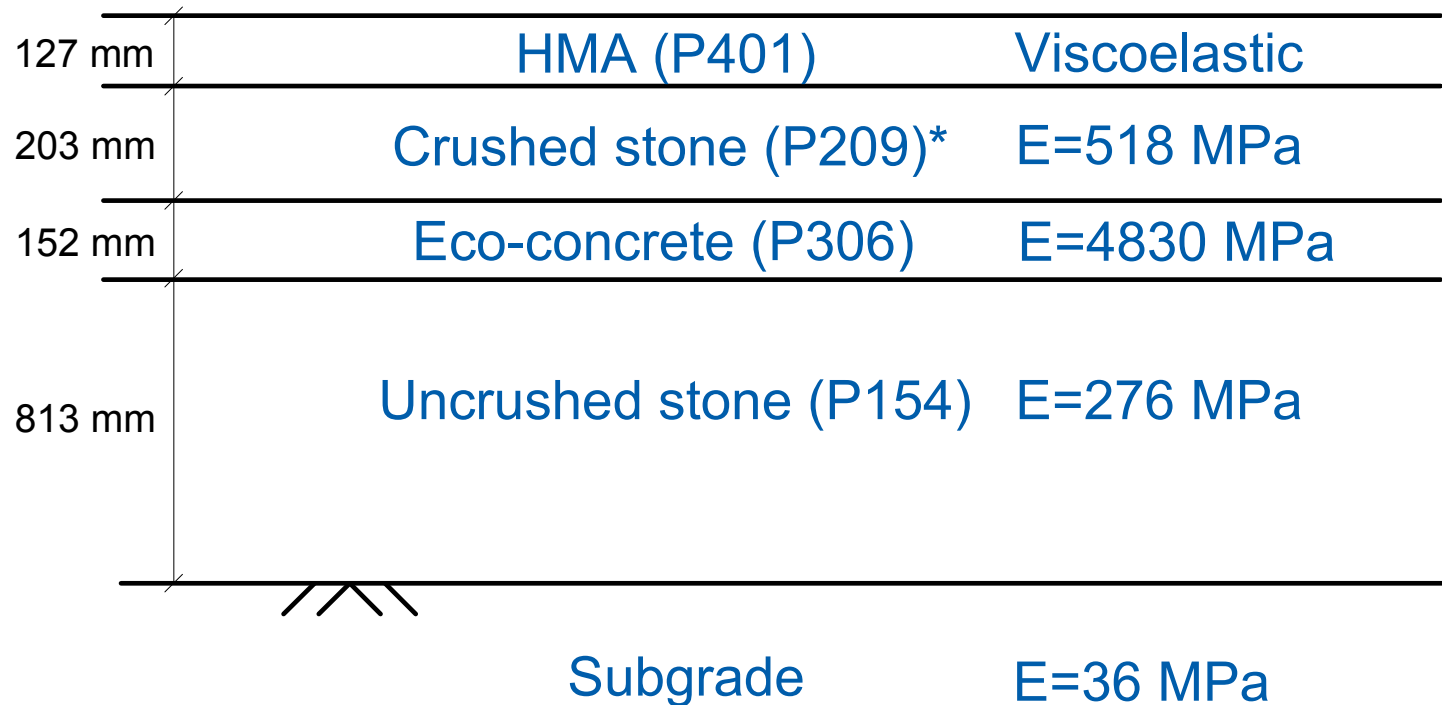


Using static uniform pressure on circular area



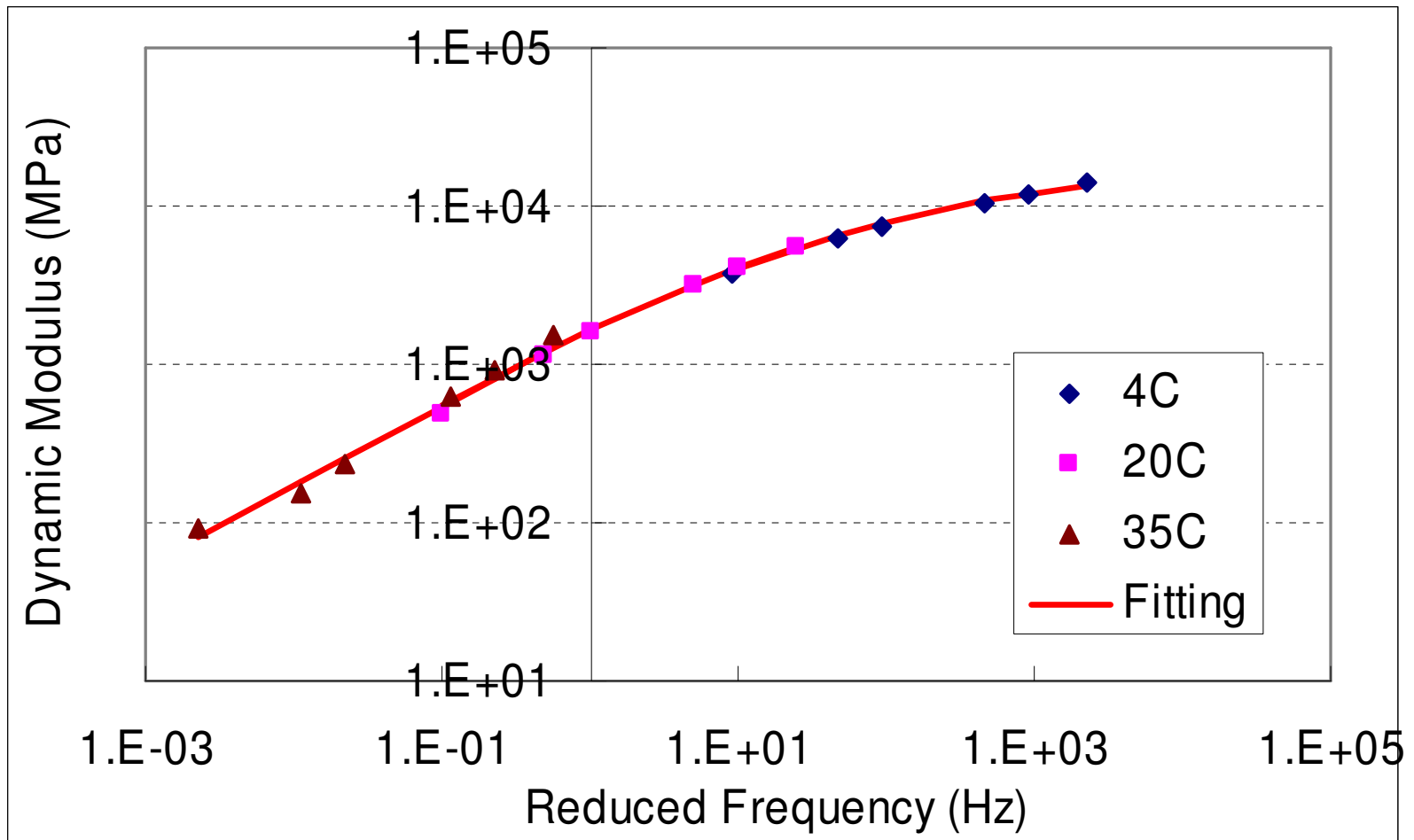
# Pavement Structure

## Pavement section considered (FAA NAPTF)



\* P154 was also used to evaluate the effect of base support

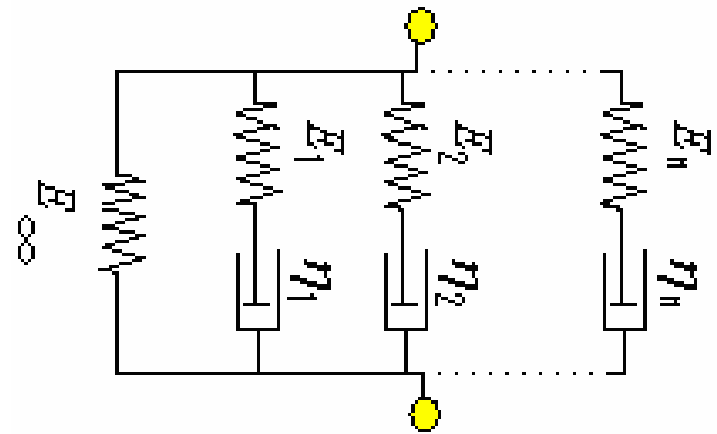
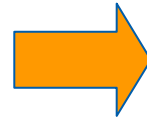
# HMA Dynamic Modulus



# HMA Linear Viscoelasticity

- **Generalized Maxwell Solid Model: Consists of one spring and n Maxwell elements connected in parallel**

$$E(t) = E_0 \left( 1 - \sum_{i=1}^N E_i (1 - e^{-t/\tau_i}) \right)$$



where,

$E(t)$  is relaxation modulus;

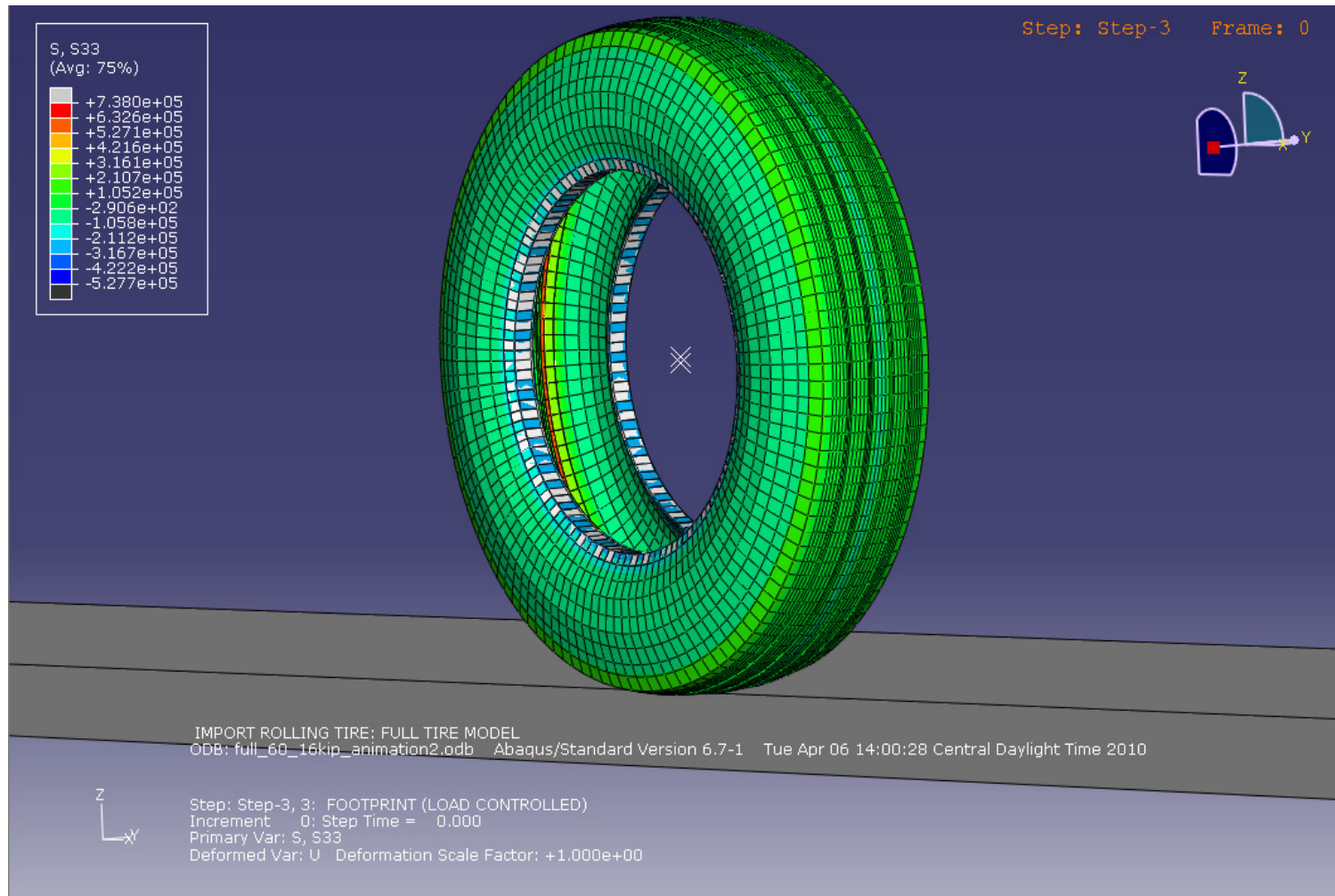
$E_0$  is instantaneous modulus;

$E_i$  and  $\tau_i$  are Prony series parameters; and

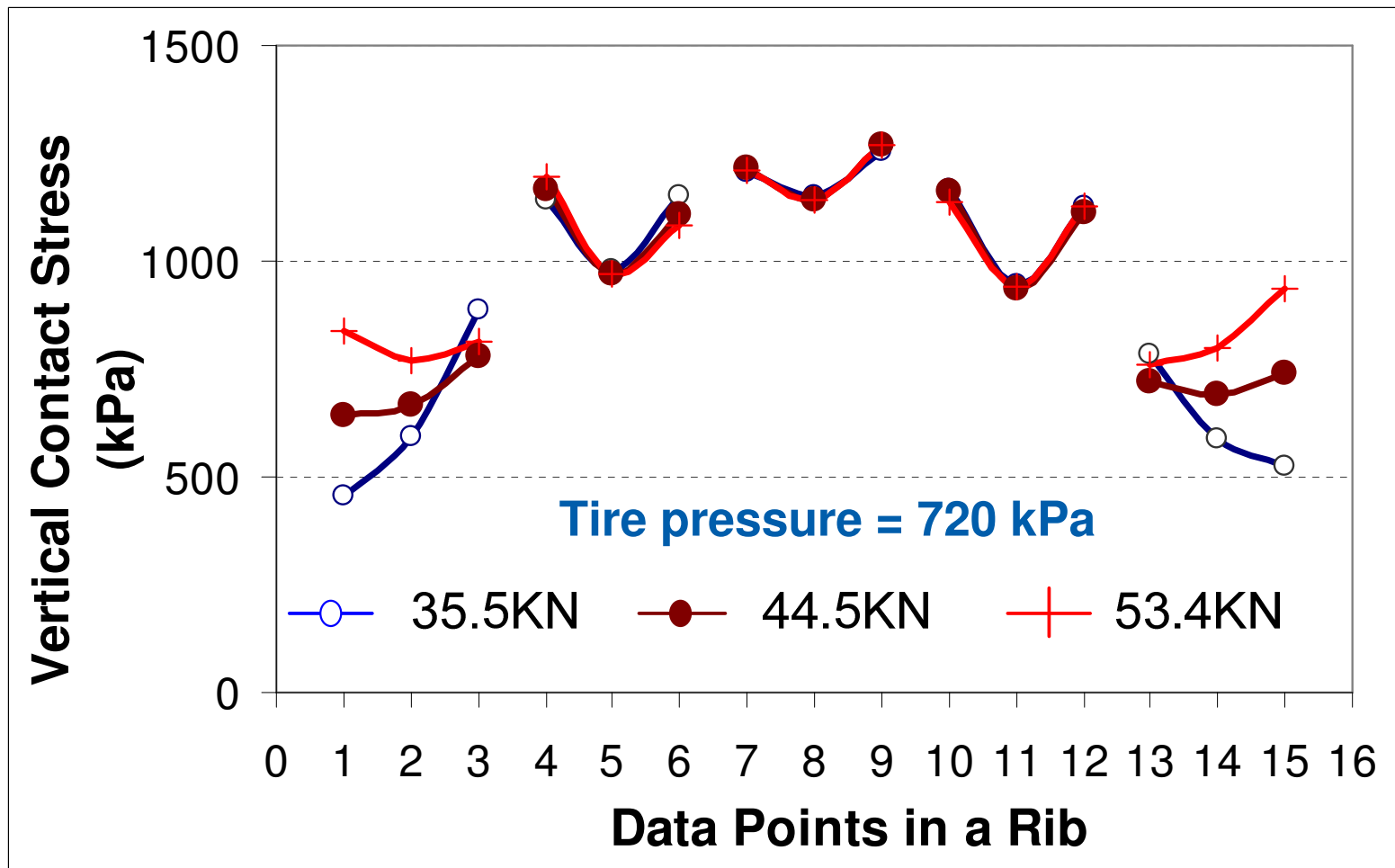
$t$  is relaxation time.

- **Relaxation modulus is converted from dynamic modulus and expressed as Prony Series**

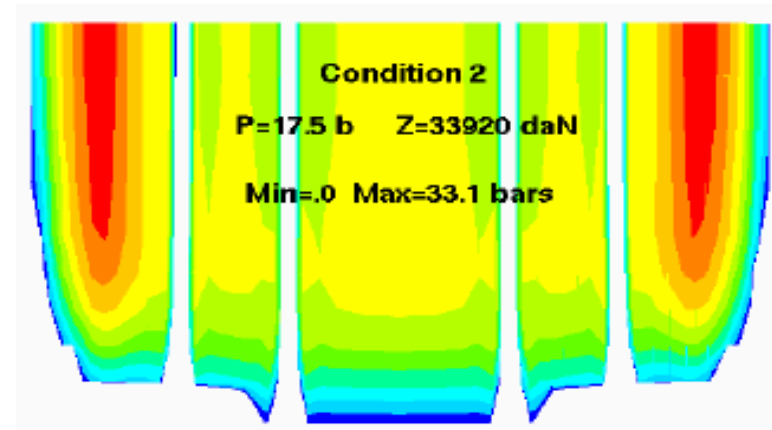
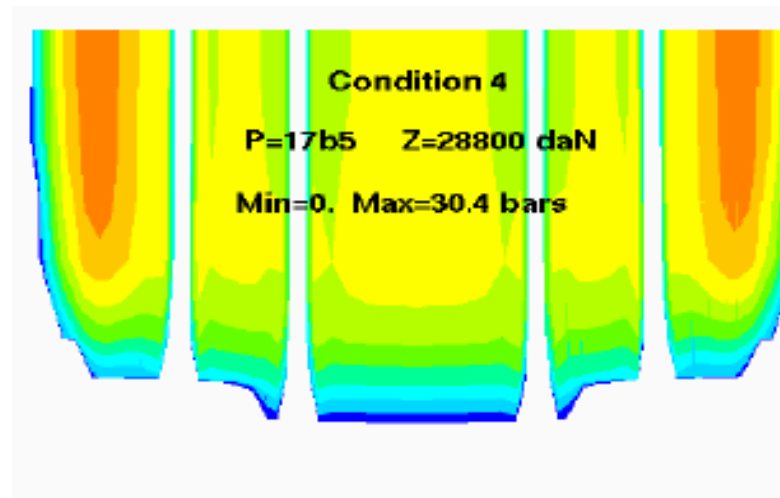
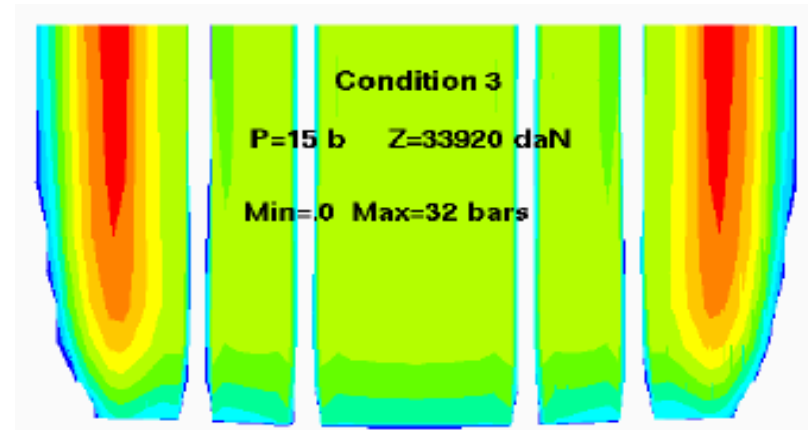
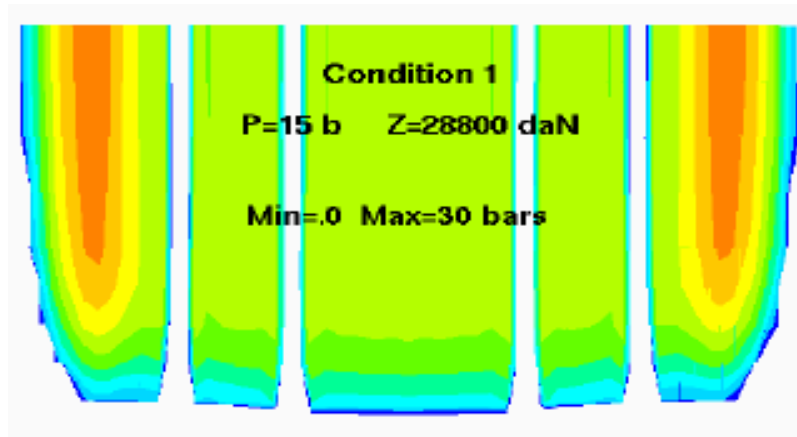
# Tire Deformation under Wheel Load



# Changes in Contact Pressure under Loading (Truck Tire)



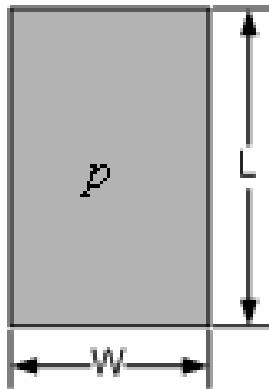
# Changes in Contact Pressure under Loading (High Aircraft Tire Load)



(After E. Rolland Michelin)

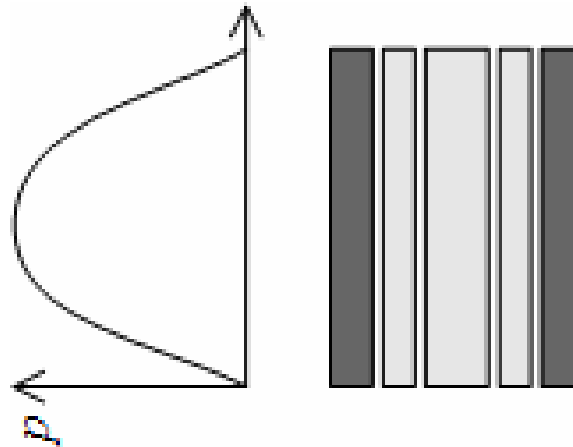
# Uniform vs. Non-uniform Contact Pressure Assumptions

- **A380 maximum takeoff weight: 560 tons**
  - Load on one main landing wheel: 260.68 kN
- **Tire inflation pressures: 15 and 17 bars**



$p$  = tire pressure  
 $W/L = 0.6 - 0.7$

**Uniform**

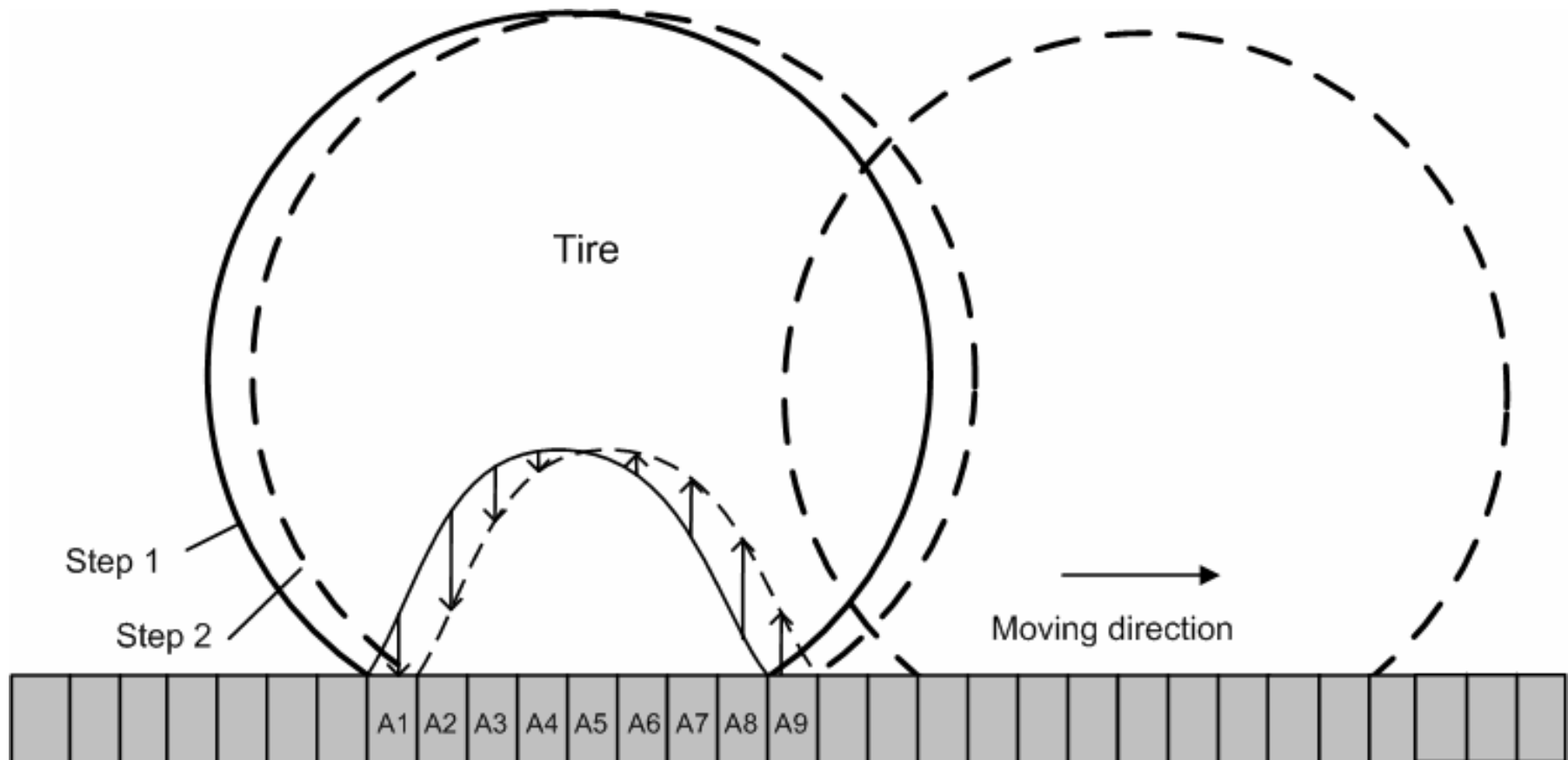


Edge ribs : peak =  $2.2 \times$  tire pressure  
Center ribs: peak =  $1.1 \times$  tire pressure

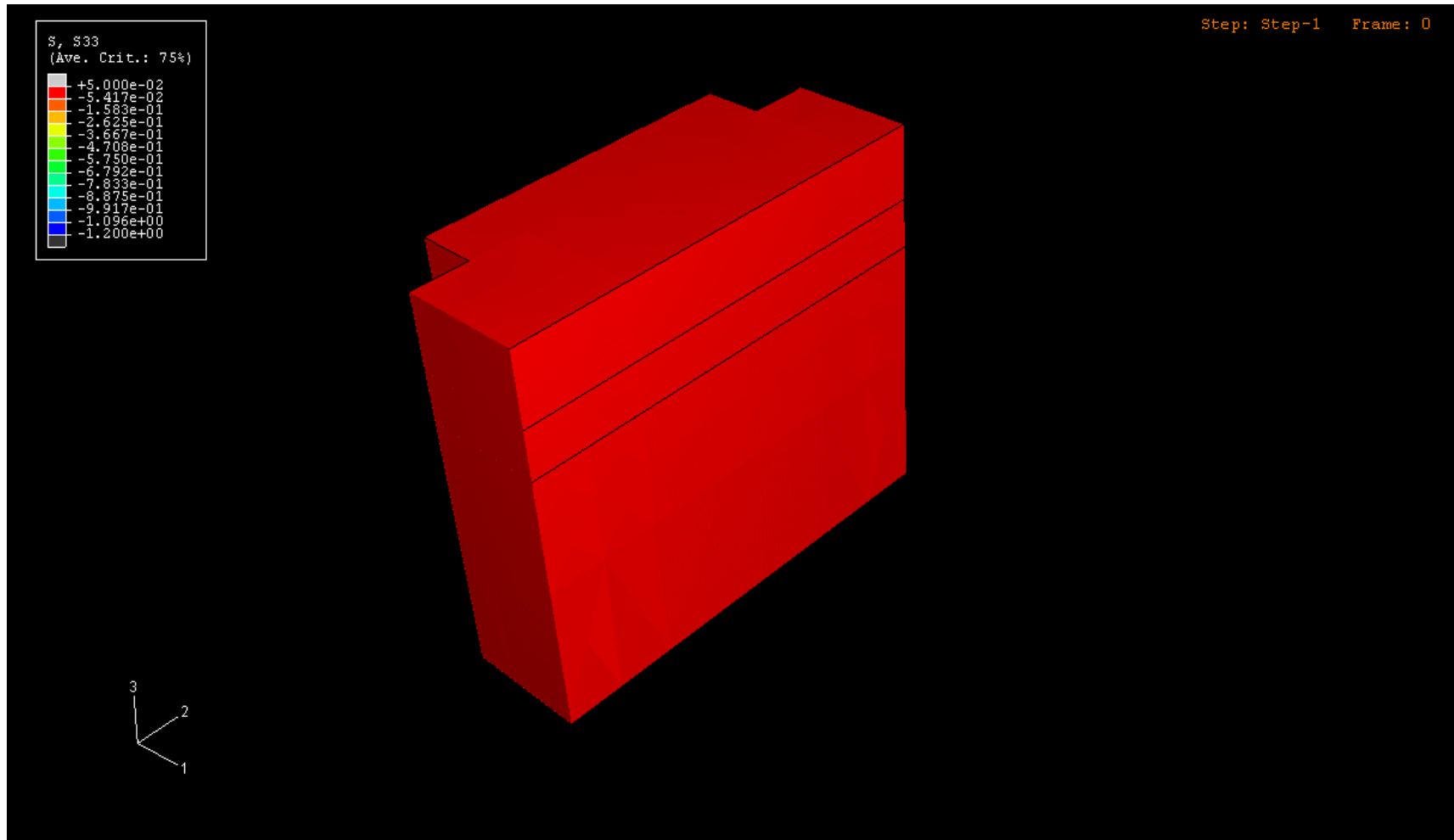
**Non-uniform**



# Moving Load Simulation



# Pavement Stress under Moving Load



# Dynamic Analysis

- **Aircraft tire loading**
  - Time (frequency)-dependent loading history
  - Dynamic amplification depends on ratio of loading frequency to pavement natural frequency

- **Dynamic analysis considers the effects of mass inertia and damping forces**

$$[M]\{\ddot{U}\} + [C]\{\dot{U}\} + [K]\{U\} = \{P\}$$

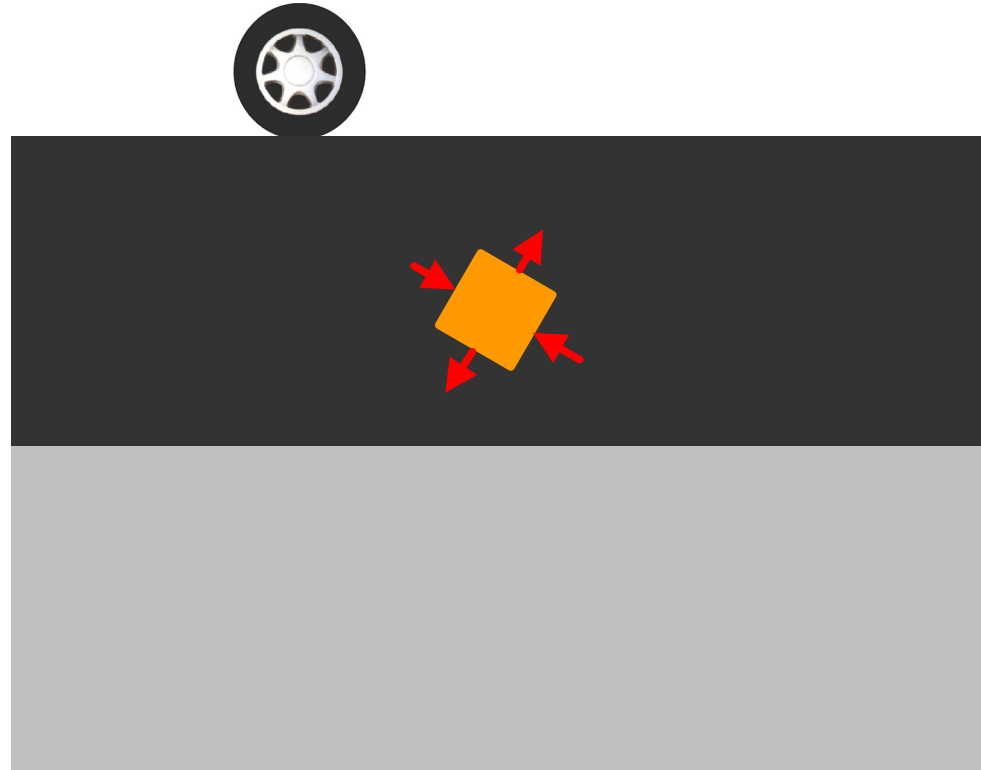
- **Implicit dynamic analysis was used**
  - More stable compared to explicit analysis
  - Efficient for structural analysis with relatively longer loading period

# Critical Pavement Responses

---

- ❑ **Mechanistic-Empirical pavement design relates critical pavement responses at specific locations to pavement damage through transfer functions**
- ❑ **Critical responses considered in this study**
  - ❑ Tensile strain at the bottom of HMA layer causing bottom-up fatigue cracking (*relatively thin HMA*)
  - ❑ Shear strain/stress in the HMA layer causing primary rutting and near-surface cracking

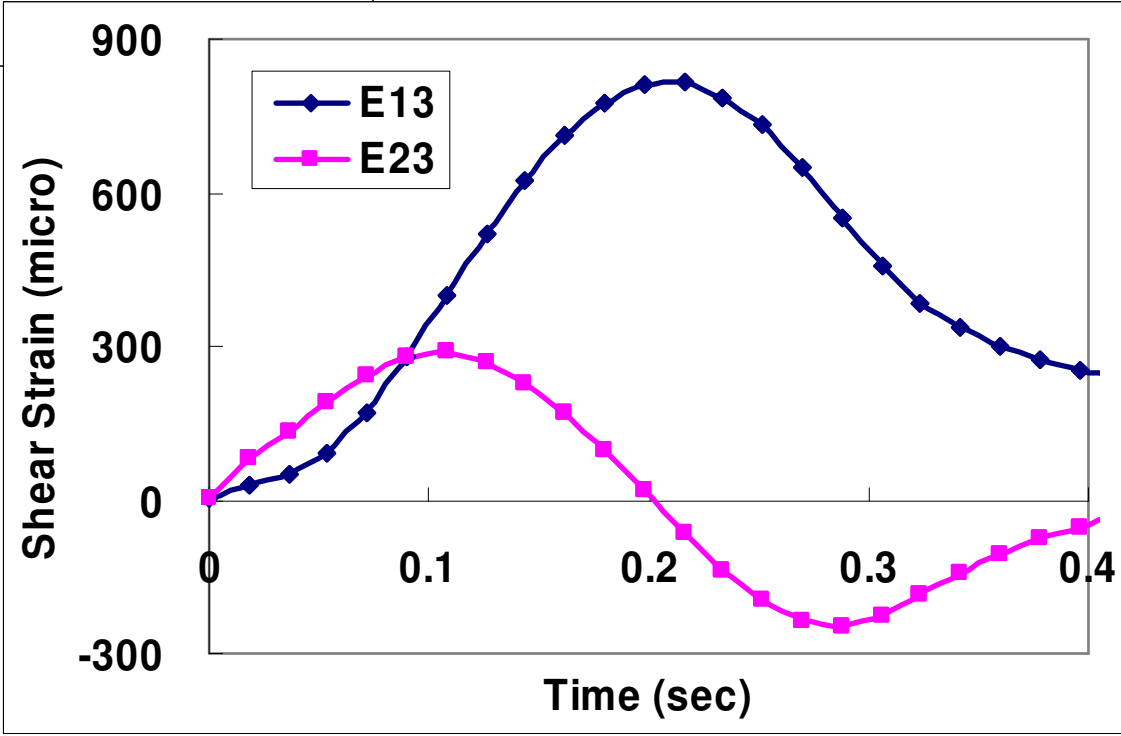
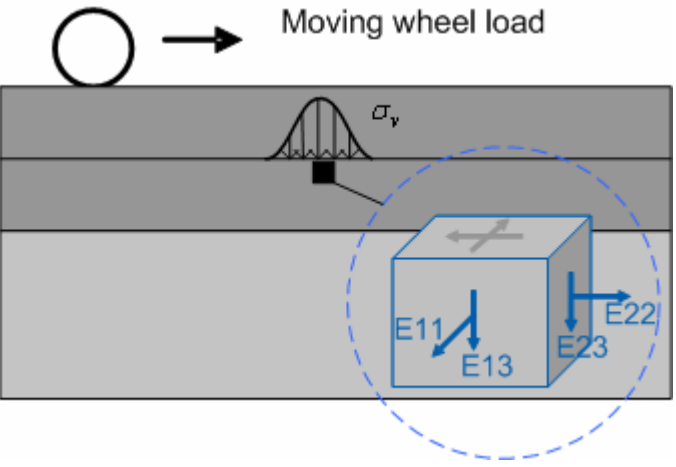
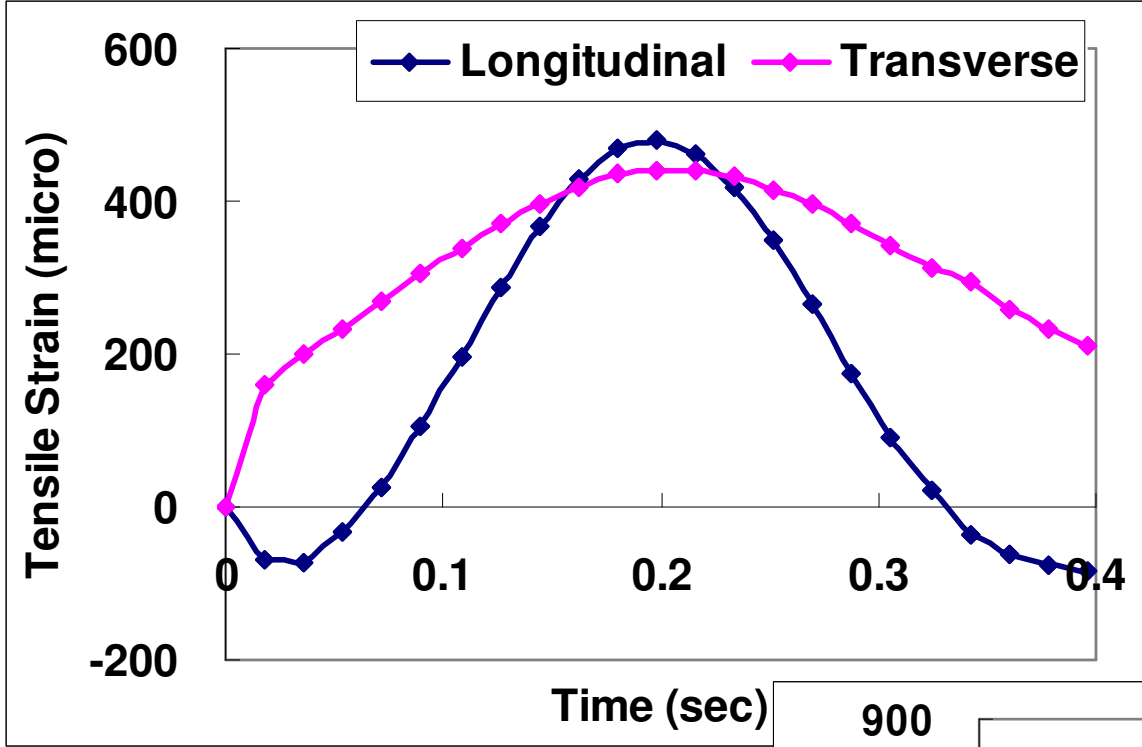
# Stress States under Moving Load



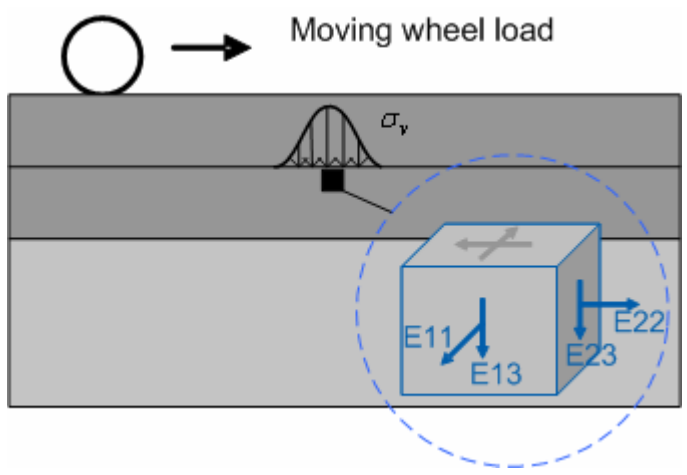
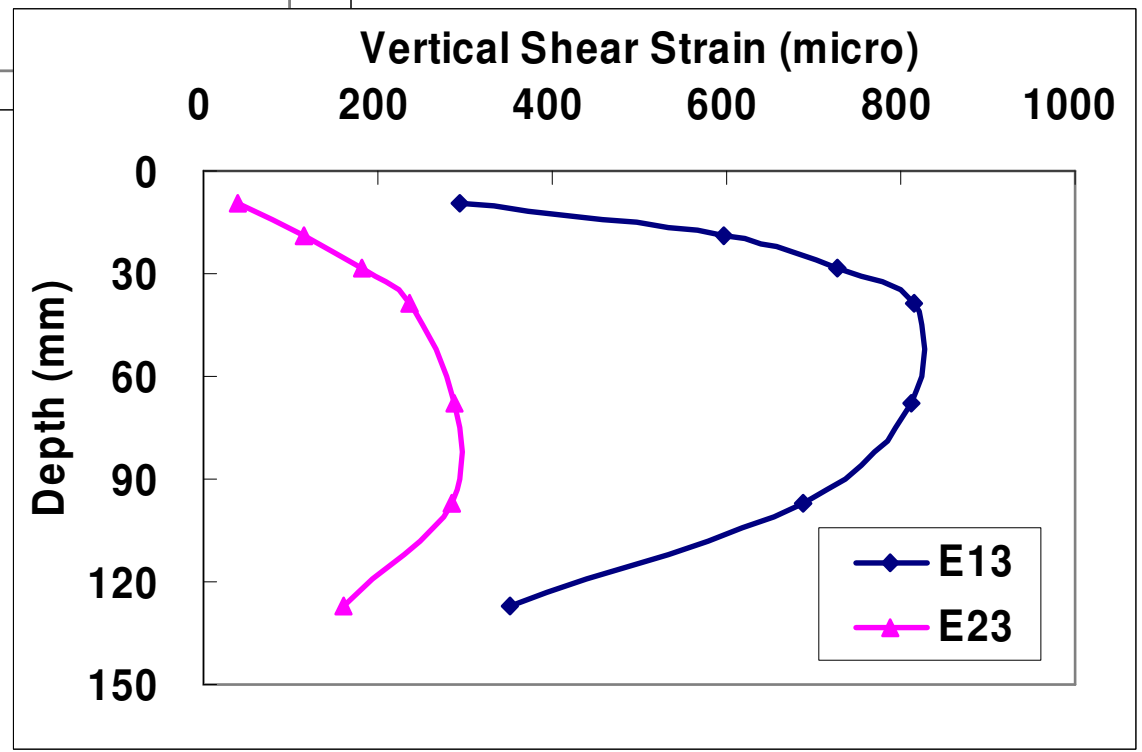
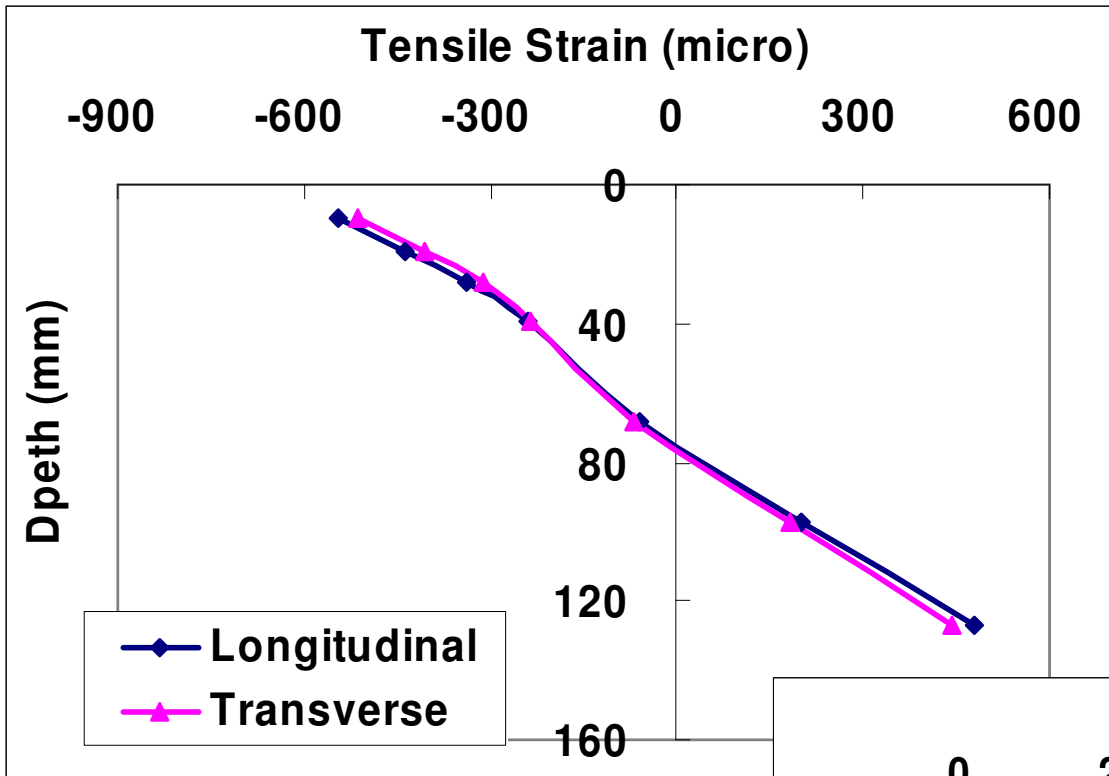
- **Principal stresses rotate** under a moving load
- **Loading time varies** at various pavement depths and directions



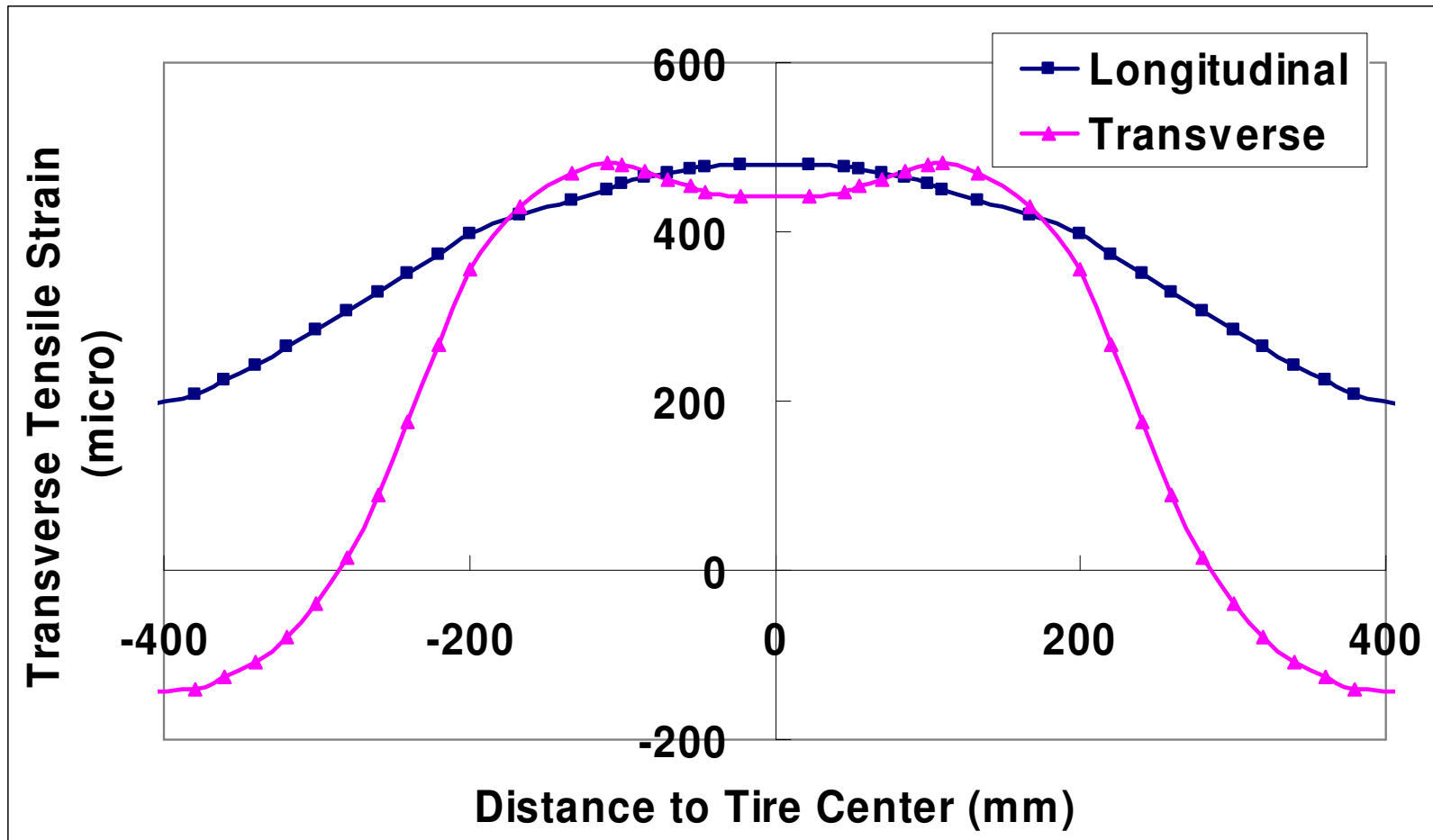
# Strains under Moving Load



# In-depth Strain Distribution



# Transverse Distribution of Tensile Strains



*(Using non-uniform contact pressure)*

# Effect of Contact Pressure Distribution

| Base material                         | Crushed stone (P209) |             |        | Uncrushed stone (P154) |             |        |
|---------------------------------------|----------------------|-------------|--------|------------------------|-------------|--------|
| Contact pressure                      | Uniform              | Non-uniform | Change | Uniform                | Non-uniform | Change |
| Transverse tensile strain ( $\mu$ )   | 493                  | 360         | -27%   | 624                    | 482         | -23%   |
| Longitudinal tensile strain ( $\mu$ ) | 251                  | 380         | +51%   | 336                    | 479         | +43%   |
| Shear strain ( $\mu$ )                | 541                  | 735         | +36%   | 680                    | 815         | +20%   |
| Shear stress (kPa)                    | 707                  | 1136        | +61%   | 818                    | 1251        | +53%   |

*(Tire pressure = 15 bar)*

# Effect of Tire Pressure

## (Using uniform contact pressure)

| Base material                         | Crushed stone (P209) |        |        | Uncrushed stone (P154) |        |        |
|---------------------------------------|----------------------|--------|--------|------------------------|--------|--------|
|                                       | Tire pressure        | 15 bar | 17 bar | Change                 | 15 bar | 17 bar |
| Transverse tensile strain ( $\mu$ )   | 493                  | 522    | +6%    | 624                    | 660    | +6%    |
| Longitudinal tensile strain ( $\mu$ ) | 251                  | 317    | +26%   | 336                    | 412    | +23%   |
| Shear strain ( $\mu$ )                | 541                  | 597    | +10%   | 680                    | 714    | +5%    |
| Shear stress (kPa)                    | 707                  | 819    | +16%   | 818                    | 942    | +15%   |

# Effect of Tire Pressure

## (Using non-uniform contact pressure)

| Base material                         | Crushed stone (P209) |        |        | Uncrushed stone (P154) |        |        |
|---------------------------------------|----------------------|--------|--------|------------------------|--------|--------|
| Tire pressure                         | 15 bar               | 17 bar | Change | 15 bar                 | 17 bar | Change |
| Transverse tensile strain ( $\mu$ )   | 360                  | 377    | +5%    | 482                    | 492    | +2%    |
| Longitudinal tensile strain ( $\mu$ ) | 380                  | 443    | +17%   | 479                    | 532    | +11%   |
| Shear strain ( $\mu$ )                | 735                  | 811    | +10%   | 815                    | 893    | +10%   |
| Shear stress (kPa)                    | 1136                 | 1307   | +15%   | 1251                   | 1428   | +14%   |



# Summary

---

- **The developed 3-D FE model can capture the distributions of tensile and shear strains under various moving tire loads**
- **High aircraft tire pressure and non-uniform contact stresses at tire-pavement interface cause high shear strains/stresses in the asphaltic mix layer**
  - Responsible for primary rutting and near-surface cracking
  - This requires high stability and shear strength asphalt mixtures

## Summary (Cont'd)

---

- **Compared to uniform contact stresses, non-uniform contact stresses under high aircraft tire pressure results in**
    - Longitudinal tensile strain increase up to 50%
    - Shear stress/strain increase up to 60%
  - **The increase of tire pressure from 15 to 17 bars results in**
    - Tensile strain increase up to 20%
    - Shear stress/strain increase up to 15%
- These changes are contact stress distribution and pavement layer stiffness dependednt**



# Acknowledgement

---

- ❑ **National Center for Supercomputing Applications (NCSA) at UIUC**
- ❑ **Jeffrey Gagnon and Navneet Garg of FAA**
- ❑ **Earlier work by Pyeong Jun Yoo (KICT) and Mostafa Elseifi (LSU)**

Thank You  
Questions ?



UNIVERSITY OF **ILLINOIS**  
AT URBANA-CHAMPAIGN